

Enhancing qubit readout with Bayesian Learning

F. Cosco^{1,*} and N. Lo Gullo^{2,3,1,†}

¹Quantum algorithms and software, VTT Technical Research Centre of Finland Ltd, Tietotie 3, 02150 Espoo, Finland

²Dipartimento di Fisica, Università della Calabria, 87036 Arcavacata di Rende (CS), Italy

³INFN, Sezione LNF, gruppo collegato di Cosenza

We introduce an efficient and accurate readout measurement scheme for single and multi-qubit states. Our method uses Bayesian inference to build an assignment probability distribution for each qubit state based on a reference characterization of the detector response functions. This allows us to account for system imperfections and thermal noise within the assignment of the computational basis. We benchmark our protocol on a quantum device with five superconducting qubits, testing initial state preparation for single and two-qubits states and an application of the Bernstein-Vazirani algorithm executed on five qubits. Our method shows a substantial reduction of the readout error and promises advantages for near-term and future quantum devices.

I. INTRODUCTION

The promises of quantum computing as a revolutionary technology are being challenged by severe technological limitations in the current hardware. The noise level in the single and two-qubit gates is undoubtedly one such factor [1], if not the most important one at the moment.

On the one hand, this prevents the building of fault-tolerant quantum computers and makes the current noisy intermediate-scale quantum (NISQ) processing units of limited use, especially when compared with classical (super-)computers. On the other hand, these limitations are fostering the emergence of new research aiming at exploiting these devices as they are [2–4], not seeing them as a first rough attempt towards a fully fault-tolerant quantum computer. Possible solutions come from improving the design of quantum processing units [5] to improving the control electronics, from increasing manufacturing quality to creating algorithms and software to optimize the data pre/post-processing.

Quantum error mitigation is a general framework grouping all techniques that aim to improve the performances of NISQ processing units [7–11], typically by post-processing the data of the quantum computation to decrease noise impact [12, 13]. Recently limitations of QEM have been shown [14, 15].

In a quantum processor, errors arise at all different stages of computation alike in a classical one: i) when loading data (state preparation); ii) during data processing (circuit execution); iii) at the moment of the readout (measurement). Most of the focus has been on mitigating errors at the level of the quantum circuit execution, e.g. zero noise extrapolation [16–20]. Recently, several works have focused the attention on improving the readout fidelity [21–33], thus reducing the error which is still very large ($\approx 1 - 2\%$ in the best cases). Such a large error alone is enough to prevent from exploiting the potential

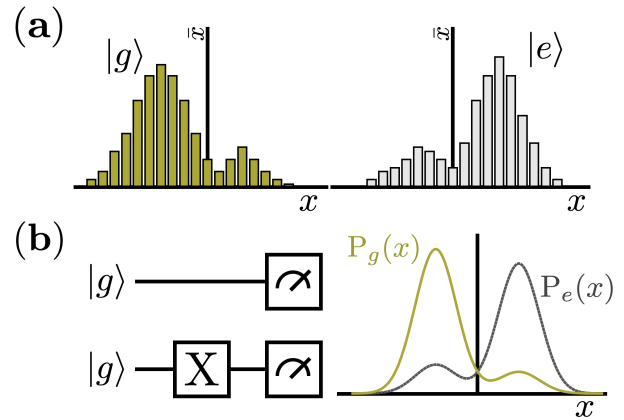


Figure 1. (a) Pictorial representation of typical qubit-state-dependent response functions, i.e. distribution of the physical values collected by the detector when the qubit is in the ground or excited state. (b) Sketch of the calibration protocol step. We collect the data when the qubit is in its ground state and its excited state, after applying an X-gate. The collected data are used to fit the response functions $P_g(x)$ and $P_e(x)$.

of quantum computers either in their NISQ version or, even worse, if we aim at error correcting algorithms.

The approaches to improve the readout fidelity include a series of techniques spanning from improving the pulse protocol before the measurement to the post-processing of the counts. Some proposals to improve the discrimination between the two states, which are gaining attention, are based on machine learning-based techniques [12], either in post-processing or during the readout protocol [34–36].

In this work, we introduce a statistical readout framework based on Bayesian inference, inspired by successful application of Bayesian inference in quantum metrology and sensing [37, 38] or parameter estimation for quantum circuits and states [39–43]. Our Bayesian Learning Readout (BaLeRO) relies upon two steps: i) characterization of the readout device to build the detector re-

* francesco.cosco@vtt.fi

† nicolino.logullo@unical.it

sponse functions; ii) post-processing data obtained from the circuit execution using a Bayesian update rule and the functions obtained from the first step. Moreover, the post-processing algorithm's input is the raw data from the detector (e.g. quantum analyzer), and the output is some probability distribution for the occupation of the computational basis (e.g. for a single qubit $|0\rangle$ and $|1\rangle$). Crucially, this approach is not a single-shot discriminator but leverages all measurement data to reconstruct the system density matrix. We will show that with our algorithm, one can improve the results obtained on actual quantum processing units for a series of quantum circuits and algorithms. Albeit we primarily focus and perform our tests on a superconducting qubit device, the approach could be applied to other platforms which allow for the reconstruction of the readout device response functions.

II. EMBRACE THE NOISE

In a quantum computer, a qubit is encoded into two (often energy) levels of a physical system whose energy spectrum typically includes many more levels. Thus, the state of the qubit is described by two orthogonal states $|g\rangle$ (ground) and $|e\rangle$ (excited) which are assigned to the computational states 0 and 1. Any readout protocol aims at discriminating between these two states. Specifically, when the qubit is prepared in the generic state $|\psi\rangle = \alpha_g|g\rangle + \alpha_e|e\rangle$ a measurement performed in the computational basis will find the system in $|g\rangle$ or $|e\rangle$ with probabilities $\rho_g = |\alpha_g|^2$ and $\rho_e = |\alpha_e|^2$, often referred as populations. In practice, each circuit run will yield one of the two outcomes commonly known as counts, which are aggregated and divided by the number of shots, i.e. repetitions, in order to obtain an estimation of ρ_g and ρ_e . In the multi-qubits case, the readout is applied to each qubit independently and the aggregation leads to the probabilities of multi-qubits states (bit-strings).

In a superconducting qubits device, each qubit is dispersively coupled to a resonator. Thus, driving the resonator results in distinct responses when the qubit is in the ground or excited state [44]. In the ideal case, we want the detector to distinguish the two phases unambiguously. However, in a real system, due to a multitude of external and possibly uncontrollable factors, such as imperfections in the system Hamiltonian, faults in the readout of the resonator, or thermal fluctuation of the system, the response of the detector will include uncertainty in the assignment of the qubit state.

Indeed, instead of getting two expected sharp signals depending on the two possible states of the qubit, the typical response function of a detector is more similar to the one in Fig. 1 (a).

A standardised readout scheme usually defines a separatrix in between the two distribution in order to discriminate between the two states in each single-shot experiment. Since the response distributions are not completely

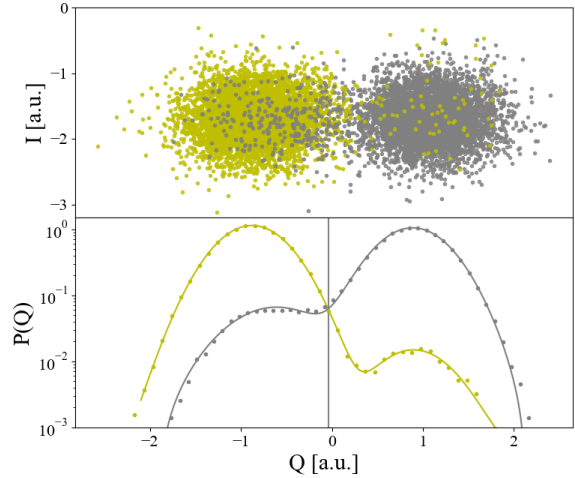


Figure 2. (Top panel) Measurement clouds in IQ plane. (Bottom panel) Collapsed histograms and fitted response functions of IBM Quito Q4.

separated, as in Fig. 1 (a), the assignment fidelity will never reach unity even in the limit of infinite repetitions. This is true even in the case the separatrix is defined in the two-dimensional plane of the I-Q signals and/or in the case one adopts more complex protocols.

To mitigate these issues, we develop a radically different approach to the problem, which *embeds* the base noise into the assignment process. We achieve the goal in two steps: i) we fully characterize the detector by building the response functions $P_g(x)$ and $P_e(x)$ for each qubit, i.e. the probability of measuring the physical value x when the qubit is in the ground and excited state respectively; ii) we use this information for post-processing the data after the execution of a generic quantum circuit through a Bayesian-like update rule.

During the first step, one builds a model for the two distributions by performing two simple experiments: reset of the qubit and readout; flip of the qubit to the excited state and readout; both these distributions are typically well represented by bimodal Gaussian distributions.

The post-processing step relies on the probabilistic relation between the value x of a physical quantity, e.g. voltage, registered in a single measurement and the state of the qubit,

$$P(x|\rho_g, \rho_e) = \rho_g P_g(x) + \rho_e P_e(x), \quad (1)$$

which can be formally interpreted as the probability of measuring the value x given a quantum state with populations ρ_g and ρ_e . Contrarily to the common approach, our algorithm leverages Eq. (1) and the full set of measurement outcomes $\mathbf{x} = x^{(1)}, \dots, x^{(N_{\text{shots}})}$ from the detector in order to build a probability distribution for the population of each state consistent with the collected raw

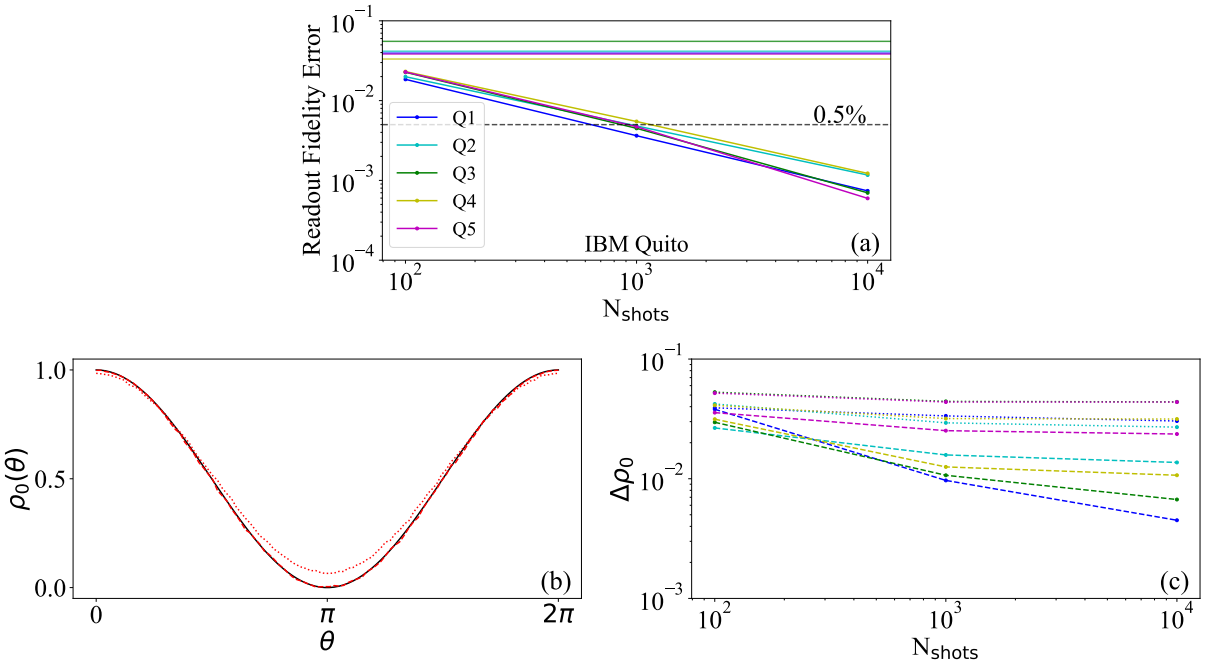


Figure 3. (a): Mitigated Readout fidelity error as a function of the number of shots for each superconducting qubit on IBM Quito. The horizontal lines correspond to the fidelity for the counts reported by the service provider (in the appropriate color scheme for each qubit). (b): Ground state population of Q1 after applying a $R_y(\theta)$ gate. The solid black line correspond to the theoretical exact population, i.e. $\cos(\theta/2)^2$, the dotted line to the counts estimate and the dashed to the values estimated trough BaLeRO with 10^4 shots. (d): average ground-state population error, $\Delta\rho_0 = 1/(2\pi) \int d\theta |\cos(\theta/2)^2 - \rho_0(\theta)|$ as a function of the number of shots for each qubit, dotted lines refer to the counts estimates and the dashed to the post-processed estimates (the colour scheme is the same as in (a)).

measurement data, i. e. $P(\rho_g, \rho_e | \mathbf{x})$. This is achieved through a Bayesian update rule

$$P(\rho_g, \rho_e | x^{(n)}) \propto \left[\rho_g P_g(x^{(n)}) + \rho_e P_g(x^{(n)}) \right] P(\rho_g, \rho_e), \quad (2)$$

where $P(\rho_g, \rho_e)$ is the prior probability distribution and it is updated after each n -th iteration step with the posterior probability distribution $P(\rho_g, \rho_e | x^{(n)})$. When assuming no prior knowledge about the probability distribution, we start the iteration with a uniform $P(\rho_g, \rho_e)$. The iteration cycle allows building a probability distribution for the qubit populations from which we can obtain an estimate, as $\bar{\rho}_{g/e} = \int d\rho_g d\rho_e \rho_{g/e} P(\rho_g, \rho_e | \mathbf{x})$.

The method is not limited to single-qubit readout, but it can be applied to any multi-qubit systems following similar steps. Given a system of N_q qubits, and N_q independent detectors registering the set of measurement outcomes $\mathbf{x} = x_1, \dots, x_{N_q}$, the multi-dimensional response function will now depend on the population of each multi-qubit state and can be given as

$$P(\mathbf{x} | \rho) = \sum_i \rho_i P(\mathbf{x} | \rho_i), \quad (3)$$

where ρ_i is the population of the i -th state, e.g. $|\rho_0\rangle = |0\dots0\rangle$, $|\rho_1\rangle = |0\dots1\rangle$ up to $|\rho_{2^{N_q}-1}\rangle = |1\dots1\rangle$, and

$P(\mathbf{x} | \rho_0) = P_g(x_1)P_g(x_2)\dots P_g(x_{N_q})$ and so forth. The posterior probability distribution for the population of each state, ρ_i , can be then reconstructed in a sequence of n single-shot measurements following the Bayes' theorem as previously introduced

$$P(\rho | \mathbf{x}^{(n)}) \propto \sum_i \rho_i P(\mathbf{x}^{(n)} | \rho_i) P(\rho_i | \mathbf{x}^{(n-1)}), \quad (4)$$

within the parameters space which satisfy $\sum_i \rho_i = 1$. It is worth mentioning that our approach shares some similarities with the Iterative Bayesian Unfolding, which is a form of regularized matrix inversion applied to the response matrix [45, 46]. Here, we bypass the faulty state-assignment step and work on the continuous space of the physical measurement.

III. CALIBRATION AND IMPROVEMENT OF READOUT FIDELITIES

We test our readout scheme on a five-qubits quantum computer, the IBM Quito. We start by calibrating the reference response functions by running the circuits depicted in Fig. 1 (b) for $N_{\text{shots}} = 10^5$. A typical outcome is the one displayed in Fig. 2 (top panel) where each

measurement is represented by a dot in the I-Q plane. The clouds are then often rotated and collapsed onto one of the axis to obtain the distributions shown in Fig. 2 (bottom panel). From them we then fit the probability distributions $P_g(x)$ and $P_e(x)$ using bimodal Gaussians. We repeat the calibration procedure for each qubit on the device and then use the obtained response functions to analyse the assignment fidelity in subsequent experiments. In Fig. 3 (a), we show the average error related to the readout assignment error for each qubit as a function of the number of shots using BaLeRO. Interestingly, we are able to attain a readout error below 0.5% already below 10^4 shots, significantly improving the readout error provided by the manufacturer which is typically of the order of $\lesssim 5\%$. Strikingly increasing the number of shots improves the readout fidelity. The latter is usually insensitive to the repetitions in the computation and depends only on the calibration of the device.

To show the effect of our approach on a single-qubit gate we apply a $R_y(\theta)$ one, i.e. a rotation around the Y axis which, when applied to the ground state, results in the final populations $p_0 \equiv \rho_g = \cos(\theta/2)^2$ and $p_1 \equiv \rho_e = \sin(\theta/2)^2$. The results are reported in Fig. 3 (b). Interestingly, our method outperforms the standard readout scheme as it follows the theoretical result more closely. We quantify our protocol performances by displaying the average over θ of the error on the rotated ground state population as a function of the number of shots in Fig. 3 (c). For any number of shots and for each qubit, our protocol achieves a smaller error than the standard (non-mitigated) case. The error on the gate for the non-mitigated case shows some improvement with increasing number of shots, saturating around 10^4 shots. Nonetheless, our approach shows a dramatic improvement for all qubits on average.

IV. MULTI-QUBIT USE-CASES AND SCALABILITY

A typical quantum algorithm requires to compute mean values of multi-qubits observables. In this section, we show how to apply the BaLeRO approach to compute such mean values and apply it to specific algorithms. As a simplest extension let us consider the preparation of a Bell state $|\Phi^+\rangle = 1/\sqrt{2}(|00\rangle + |11\rangle)$. In Fig. 4 (a), we display the total population error calculated using our method and the standard discriminator methods for each qubit pair prepared in the Bell state $|\Phi^+\rangle$. For each qubit pair, our protocol outperforms the count statistics. As an example, in Fig. 4 (b), we compare the populations of one of the experiments.

In many practical applications, having access to an accurate description of the two-qubit density matrix is crucial. For example, the calculation of ground state properties of many-body systems, such as spin chains, require, at most, two-body operators. This applies also for simple molecular systems or ferromagnetic models [47], which

after "qubitization" have an Hamiltonian with at most two-body operators. As proof of principle, we consider the H_2 molecule, whose ground state energy can be calculated through a simplified two-qubits system [48, 49]. In Fig. 4 (c), we show the lower energy extracted by using the state preparation ansatz, and Hamiltonian data, of [27] for $N_{shots} = 10^3$. Even in this case our method outperforms the non-mitigated one confirming that the error on the readout is a significant limiting factor in current devices.

Up to two-qubit quantities, the post-processing algorithm is computationally inexpensive. However, the computational cost increases rapidly, actually exponentially, with the number of qubits making it unfeasible. As an example, for a system with N_q qubits, Eq. (4) requires handling, at each iteration step of the learning, a multi-parameter probability distribution $P(\rho|x^{(n)})$ where each variable, i.e. the 2^{N_q} different populations ρ_i , is sampled in the interval $[0, 1]$. If each interval is sampled simultaneously with n_p points, the total probability distribution would require a mesh-grid with $n_p^{2^{N_q}}$ points, albeit the normalisation condition reduces the effective number of independent coordinates.

Therefore, it appears quite clearly how in the multi-qubit scenario our approach is resource intensive and cannot be used as it is, and it requires to be adapted.

Therefore, we follow an heuristic approach and instead of working with the complete multi-parameter probability distribution we demote all the populations except two, namely ρ_i and ρ_j , to constant estimates R_k and define the conditional probability function

$$P(\mathbf{x}|\rho_i, \rho_j) = \rho_i P(\mathbf{x}|\rho_i) + \rho_j P(\mathbf{x}|\rho_j) + \sum_{k \neq i, j} R_k P(\mathbf{x}|R_k). \quad (5)$$

Using this, we apply the Bayesian cycle to build a posterior distribution for the population pair in exam, which is then used to compute some new estimates R_i and R_j . The algorithm needs to be repeated for each population pair (ρ_i, ρ_j) and iterated to reach convergence. The convergence criterion can be chosen at will; a simple rule of thumb is to stop the iterations if the change in the posterior probabilities or the obtained populations does not change with respect to the previous iteration by an amount ϵ .

To further lighten the computational cost, we reduce the number of parameters ρ_i included in the optimization procedure. The strategy is to use the initial estimates R_k , which at the beginning can be the result obtained via the count statistics, to drop states which have a negligible population according to a pre-defined threshold. In our test we drop from the optimization the states for which we do not get initial counts.

While a highly entangled many-qubit state might still be difficult to reconstruct, we applied our protocol to a quantum algorithm whose theoretical output is a single bitstring, i.e. the Bernstein-Vazirani algorithm [50, 51]. In Fig. 4 (d), we compare the populations measured us-

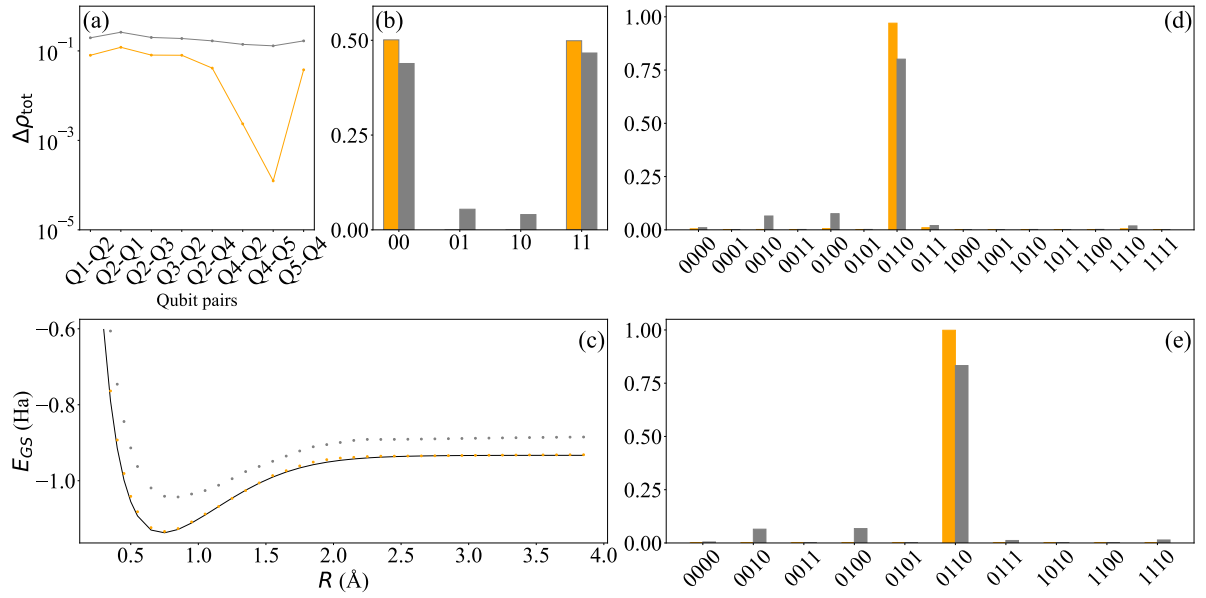


Figure 4. (a) Total population error $\Delta\rho_{\text{tot}} = \sum_i |\rho_i^{\text{exact}} - \rho_i^{\text{measured}}|$ as a function of the qubit pairs, and (b) populations of the pair Q4-Q2, for the Bell state $|\Phi^+\rangle$ measured using BaLeRO (orange) and the count statistics (gray). Each experiment is performed using $N = 10^4$ shots. (c) H_2 ground state energy measured using BaLeRO (orange) and the count statistics (gray) using 10^3 shots on pair Q1-Q2. Populations measured using BaLeRO (orange) and the count statistics (gray) in the four qubits system prepared in the state "0110" as output of the Bernstein-Vazirani Algorithm in (d) and state preparation through single qubit flips in (e), both measured with 10^4 shots.

ing our approach, with parameter region restriction and Bayesian update applied to population pairs, and the count statistics. We applied the Bernstein-Vazirani algorithm on a five qubits system to obtain the four qubits string "0110" as an output. Our protocol increases the population of the correct output string, reducing the error from $\sim 17\%$ to $\sim 3\%$. The remaining erroneous populations are mainly due to imperfections in the qubit gates. To confirm that this is the case, we prepare the same string, "0110", with a simpler circuit, i.e. by flipping the qubits. The count statistics show errors of the same order of magnitude as in the execution of the Bernstein-Vazirani algorithm (Fig. 4 (e)), while with BaLeRO we get very close to the expected outcome, reducing the error from $\sim 16\%$ to $\sim 0.15\%$.

V. CONCLUSIONS

We have introduced an efficient readout scheme, BaLeRO, which significantly improves the accuracy of the readout step in quantum computers. The algorithm employs Bayesian inference to build an assignment probability distribution for each qubit state based on a reference characterisation of the detector response functions, thus including noise and imperfections in the post-

processing of the raw measurement outcomes. We tested BaLeRO on a quantum computer with five superconducting qubits, and we have demonstrated an accuracy improvement in terms of single- and up to four-qubit readout. Although we applied the protocol to a superconducting qubit architecture, BaLeRO applies to other platforms for digital quantum computation. It is worth mentioning that BaLeRO is not a single-shot post-processing protocol based on a discriminator to assign "0" or "1" to each measurement. These approaches rely on the quality of the readout protocol itself while improving the choice of the discriminator. BaLeRO instead incorporates the readout noise in the post-processing, improving the statistical reconstruction of the quantum state coherent with the actual measurement. Finally, while already proving a reduction of the readout error as it is, embedding our scheme within the calibration process of each gate might further boost the performance of NISQ and future devices.

ACKNOWLEDGMENTS

We acknowledge the use of IBM Quantum services for this work. The views expressed are those of the authors, and do not reflect the official policy or position of IBM

or the IBM Quantum team.

[1] F. Arute, K. Arya, R. Babbush, D. Bacon, J. C. Bardin, R. Barends, R. Biswas, S. Boixo, F. G. S. L. Brandao, D. A. Buell, B. Burkett, Y. Chen, Z. Chen, B. Chiaro, R. Collins, W. Courtney, A. Dunsworth, E. Farhi, B. Foxen, A. Fowler, C. Gidney, M. Giustina, R. Graff, K. Guerin, S. Habegger, M. P. Harrigan, M. J. Hartmann, A. Ho, M. Hoffmann, T. Huang, T. S. Humble, S. V. Isakov, E. Jeffrey, Z. Jiang, D. Kafri, K. Kechedzhi, J. Kelly, P. V. Klimov, S. Knysh, A. Korotkov, F. Kostritsa, D. Landhuis, M. Lindmark, E. Lucero, D. Lyakh, S. Mandrà, J. R. McClean, M. McEwen, A. Megrant, X. Mi, K. Michelsen, M. Mohseni, J. Mutus, O. Naaman, M. Neeley, C. Neill, M. Y. Niu, E. Ostby, A. Petukhov, J. C. Platt, C. Quintana, E. G. Rieffel, P. Roushan, N. C. Rubin, D. Sank, K. J. Satzinger, V. Smelyanskiy, K. J. Sung, M. D. Tervitthick, A. Vainsencher, B. Villalonga, T. White, Z. J. Yao, P. Yeh, A. Zalcman, H. Neven, and J. M. Martinis, *Nature* **574**, 505 (2019).

[2] J. Preskill, *Quantum* **2**, 79 (2018).

[3] A. Kandala, K. Temme, A. D. Córcoles, A. Mezzacapo, J. M. Chow, and J. M. Gambetta, *Nature* **567**, 491 (2019).

[4] K. Bharti, A. Cervera-Lierta, T. H. Kyaw, T. Haug, S. Alperin-Lea, A. Anand, M. Degroote, H. Heimonen, J. S. Kottmann, T. Menke, W.-K. Mok, S. Sim, L.-C. Kwek, and A. Aspuru-Guzik, *Rev. Mod. Phys.* **94**, 015004 (2022).

[5] F. Marxer, A. Vepsäläinen, S. W. Jolin, J. Tuorila, A. Landra, C. Ockeloen-Korppi, W. Liu, O. Ahonen, A. Auer, L. Belzane, V. Bergholm, C. F. Chan, K. W. Chan, T. Hiltunen, J. Hotari, E. Hyypä, J. Ikonen, D. Janzso, M. Koistinen, J. Kotilahti, T. Li, J. Luus, M. Papic, M. Partanen, J. Räbinä, J. Rost, M. Savitskyi, M. Seppälä, V. Sevriuk, E. Takala, B. Tarasinski, M. J. Thapa, F. Tosto, N. Vorobeva, L. Yu, K. Y. Tan, J. Hassel, M. Möttönen, and J. Heinsoo, *PRX Quantum* **4**, 010314 (2023).

[6] E. Hyypä, S. Kundu, C. F. Chan, A. Gunyhó, J. Hotari, D. Janzso, K. Juliussen, O. Kiuru, J. Kotilahti, A. Landra, W. Liu, F. Marxer, A. Mäkinen, J.-L. Orgiazzi, M. Palma, M. Savitskyi, F. Tosto, J. Tuorila, V. Vadimov, T. Li, C. Ockeloen-Korppi, J. Heinsoo, K. Y. Tan, J. Hassel, and M. Möttönen, *Nature Communications* **13**, 6895 (2022).

[7] S. Endo, S. C. Benjamin, and Y. Li, *Phys. Rev. X* **8**, 031027 (2018).

[8] S. Endo, Z. Cai, S. C. Benjamin, and X. Yuan, *Journal of the Physical Society of Japan* **90**, 032001 (2021).

[9] D. Bultrini, M. H. Gordon, P. Czarnik, A. Arrasmith, P. J. Coles, and L. Cincio, *Unifying and benchmarking state-of-the-art quantum error mitigation techniques* (2021).

[10] A. Lowe, M. H. Gordon, P. Czarnik, A. Arrasmith, P. J. Coles, and L. Cincio, *Phys. Rev. Res.* **3**, 033098 (2021).

[11] Z. Cai, R. Babbush, S. C. Benjamin, S. Endo, W. J. Higgins, Y. Li, J. R. McClean, and T. E. O’Brien, *Quantum error mitigation* (2022).

[12] A. Strikis, D. Qin, Y. Chen, S. C. Benjamin, and Y. Li, *PRX Quantum* **2**, 040330 (2021).

[13] O. B. C. Y. H. E. Kim, J. and D. K. Park, *New Journal of Physics* **24**, 073009 (2022).

[14] R. Takagi, S. Endo, S. Minagawa, and M. Gu, *npj Quantum Information* **8**, 10.1038/s41534-022-00618-z (2022).

[15] Y. Kim, C. J. Wood, T. J. Yoder, S. T. Merkel, J. M. Gambetta, K. Temme, and A. Kandala, *Nature Physics* 10.1038/s41567-022-01914-3 (2023).

[16] Y. Li and S. C. Benjamin, *Phys. Rev. X* **7**, 021050 (2017).

[17] K. Temme, S. Bravyi, and J. M. Gambetta, *Phys. Rev. Lett.* **119**, 180509 (2017).

[18] T. Giurgica-Tiron, Y. Hindy, R. LaRose, A. Mari, and W. J. Zeng, in *2020 IEEE International Conference on Quantum Computing and Engineering (QCE)* (IEEE, 2020).

[19] S. J. Seo, S. and J. Bae 10.48550/ARXIV.2112.10651 (2021).

[20] M. Krebsbach, B. Trauzettel, and A. Calzona, *Phys. Rev. A* **106**, 062436 (2022).

[21] M. D. Reed, B. M. Maune, R. W. Andrews, M. G. Borselli, K. Eng, M. P. Jura, A. A. Kiselev, T. D. Ladd, S. T. Merkel, I. Milosavljevic, E. J. Pritchett, M. T. Rakher, R. S. Ross, A. E. Schmitz, A. Smith, J. A. Wright, M. F. Gyure, and A. T. Hunter, *Phys. Rev. Lett.* **116**, 110402 (2016).

[22] T. Walter, P. Kurpiers, S. Gasparinetti, P. Magnard, A. Potočnik, Y. Salathé, M. Pechal, M. Mondal, M. Oppliger, C. Eichler, and A. Wallraff, *Phys. Rev. Appl.* **7**, 054020 (2017).

[23] P. Harvey-Collard, B. D’Anjou, M. Rudolph, N. T. Jacobson, J. Dominguez, G. A. Ten Eyck, J. R. Wendt, T. Pluym, M. P. Lilly, W. A. Coish, M. Pioro-Ladrière, and M. S. Carroll, *Phys. Rev. X* **8**, 021046 (2018).

[24] B. D’Anjou and G. Burkard, *Phys. Rev. B* **100**, 245427 (2019).

[25] J. Heinsoo, C. K. Andersen, A. Remm, S. Krinner, T. Walter, Y. Salathé, S. Gasparinetti, J.-C. Besse, A. Potočnik, A. Wallraff, and C. Eichler, *Phys. Rev. Appl.* **10**, 034040 (2018).

[26] S. Touzard, A. Kou, N. E. Frattini, V. V. Sivak, S. Puri, A. Grimm, L. Frunzio, S. Shankar, and M. H. Devoret, *Phys. Rev. Lett.* **122**, 080502 (2019).

[27] M. Urbanek, B. Nachman, and W. A. de Jong, *Phys. Rev. A* **102**, 022427 (2020).

[28] L. A. Martinez, Y. J. Rosen, and J. L. DuBois, *Phys. Rev. A* **102**, 062426 (2020).

[29] F. Lecocq, F. Quinlan, K. Cicak, J. Aumentado, S. A. Diddams, and J. D. Teufel, *Nature* **591**, 575 (2021).

[30] M. R. Geller and M. Sun, *Quantum Science and Technology* **6**, 025009 (2021).

[31] J. Lin, J. J. Wallman, I. Hincks, and R. Laflamme, *Phys. Rev. Res.* **3**, 033285 (2021).

[32] L. e. a. Chen 10.48550/ARXIV.2208.05879 (2022).

[33] M. C. N. O. W. D. L. B. Maurya, S. and S. Tannu 10.48550/ARXIV.2212.03895 (2022).

[34] R. Navarathna, T. Jones, T. Moghaddam, A. Kulikov, R. Beriwal, M. Jerger, P. Pakkiam, and A. Fedorov, *Ap-*

plied Physics Letters **119**, 114003 (2021).

[35] B. Lienhard, A. Vepsäläinen, L. C. Govia, C. R. Hoffer, J. Y. Qiu, D. Ristè, M. Ware, D. Kim, R. Winik, A. Melville, B. Niedzielski, J. Yoder, G. J. Ribeill, T. A. Ohki, H. K. Krovi, T. P. Orlando, S. Gustavsson, and W. D. Oliver, *Phys. Rev. Appl.* **17**, 014024 (2022).

[36] U. Azad and H. Zhang [10.48550/ARXIV.2210.08574](https://arxiv.org/abs/2210.08574) (2022).

[37] H. T. Dinani, D. W. Berry, R. Gonzalez, J. R. Maze, and C. Bonato, *Phys. Rev. B* **99**, 125413 (2019).

[38] R. Puebla, Y. Ban, J. Haase, M. Plenio, M. Paternostro, and J. Casanova, *Phys. Rev. Appl.* **16**, 024044 (2021).

[39] B. Teklu, S. Olivares, and M. G. A. Paris, *Journal of Physics B: Atomic, Molecular and Optical Physics* **42**, 035502 (2009).

[40] S. Paesani, A. A. Gentile, R. Santagati, J. Wang, N. Wiebe, D. P. Tew, J. L. O'Brien, and M. G. Thompson, *Phys. Rev. Lett.* **118**, 100503 (2017).

[41] K. T. Laverick, I. Guevara, and H. M. Wiseman, *Phys. Rev. A* **104**, 032213 (2021).

[42] V. Gebhart, A. Smerzi, and L. Pezzè, *Phys. Rev. Appl.* **16**, 014035 (2021).

[43] B. M. Duffield, S. and R. M. [10.48550/ARXIV.2206.07559](https://arxiv.org/abs/2206.07559) (2022).

[44] A. Blais, A. L. Grimsmo, S. M. Girvin, and A. Wallraff, *Rev. Mod. Phys.* **93**, 025005 (2021).

[45] B. Nachman, M. Urbanek, W. A. de Jong, and C. W. Bauer, *npj Quantum Information* **6**, 84 (2020).

[46] R. Hicks, C. W. Bauer, and B. Nachman, *Phys. Rev. A* **103**, 022407 (2021).

[47] R. N. Tazhigulov, S.-N. Sun, R. Haghshenas, H. Zhai, A. T. Tan, N. C. Rubin, R. Babbush, A. J. Minnich, and G. K.-L. Chan, *PRX Quantum* **3**, 040318 (2022).

[48] P. J. J. O'Malley, R. Babbush, I. D. Kivlichan, J. Romero, J. R. McClean, R. Barends, J. Kelly, P. Roushan, A. Tranter, N. Ding, B. Campbell, Y. Chen, Z. Chen, B. Chiaro, A. Dunsworth, A. G. Fowler, E. Jeffrey, E. Lucero, A. Megrant, J. Y. Mutus, M. Neeley, C. Neill, C. Quintana, D. Sank, A. Vainsencher, J. Wenner, T. C. White, P. V. Coveney, P. J. Love, H. Neven, A. Aspuru-Guzik, and J. M. Martinis, *Phys. Rev. X* **6**, 031007 (2016).

[49] M. Ganzhorn, D. Egger, P. Barkoutsos, P. Ollitrault, G. Salis, N. Moll, M. Roth, A. Fuhrer, P. Mueller, S. Woerner, I. Tavernelli, and S. Filipp, *Phys. Rev. Appl.* **11**, 044092 (2019).

[50] E. Bernstein and U. Vazirani, *SIAM Journal on Computing* **26**, 1411 (1997), <https://doi.org/10.1137/S0097539796300921>.

[51] D. R. Simon, *SIAM Journal on Computing* **26**, 1474 (1997), <https://doi.org/10.1137/S00975396298637>.